LBL-12804
Preprint

Lawrence Berkeley Laboratory

UNIVERSITY OF CALIFORNIA

Materials & Molecular Research Division

Submitted to Oxidation of Metals

OXIDATION OF Fe-C ALLOYS IN THE TEMPERATURE RANGE OF 600-850°C

A.V. Malik and D.P. Whittle

April 1981

TWO-WEEK LOAN COPY

This is a Library Circulating Copy which may be borrowed for two weeks. For a personal retention copy, call Tech. Info. Division, Ext. 6782

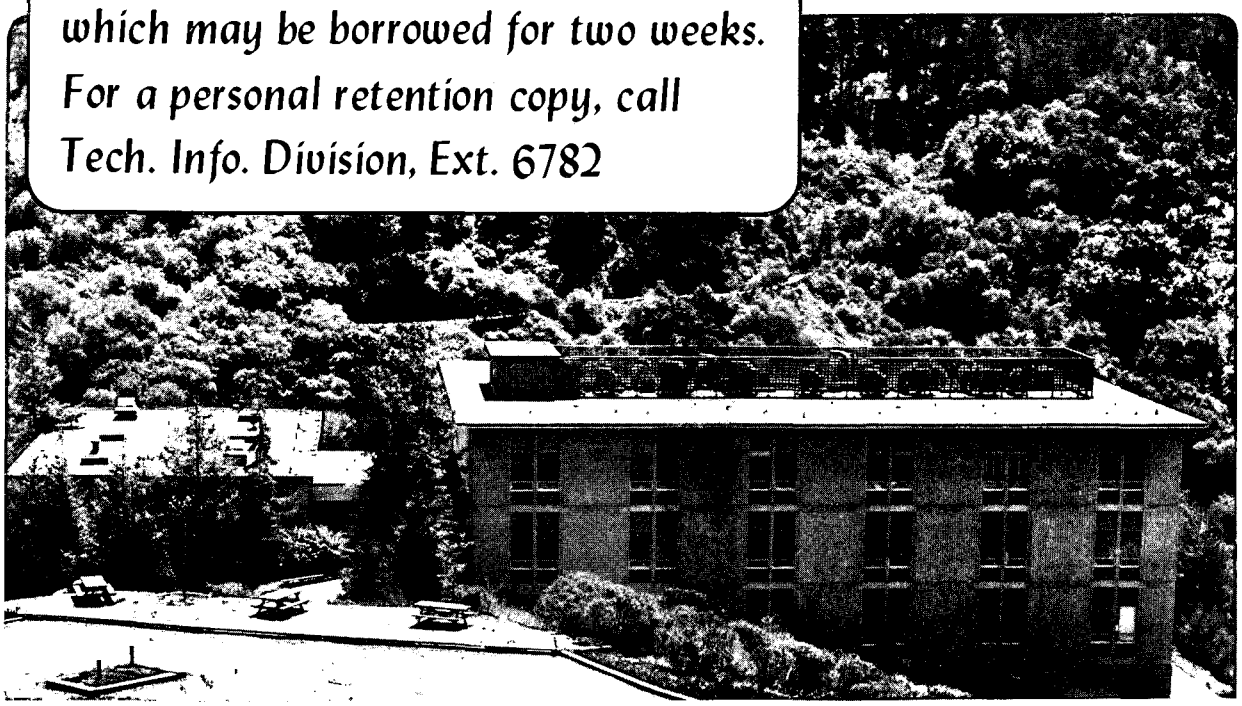

Prepared for the U.S. Department of Energy under Contract W-7405-ENG-48

LBL-12804 c.2

DISCLAIMER

This document was prepared as an account of work sponsored by the United States Government. While this document is believed to contain correct information, neither the United States Government nor any agency thereof, nor the Regents of the University of California, nor any of their employees, makes any warranty, express or implied, or assumes any legal responsibility for the accuracy, completeness, or usefulness of any information, apparatus, product, or process disclosed, or represents that its use would not infringe privately owned rights. Reference herein to any specific commercial product, process, or service by its trade name, trademark, manufacturer, or otherwise, does not necessarily constitute or imply its endorsement, recommendation, or favoring by the United States Government or any agency thereof, or the Regents of the University of California. The views and opinions of authors expressed herein do not necessarily state or reflect those of the United States Government or any agency thereof or the Regents of the University of California.

OXIDATION OF Fe-C ALLOYS IN THE TEMPERATURE RANGE OF 600-850°C

A. V. Malik[+] and D. P. Whittle*

* Lawrence Berkeley Laboratory
Department of Materials Science and Mineral Engineering
University of California
Berkeley, California 94720

ABSTRACT

The oxidation behavior of Fe-C alloys in the temperature range 600-850°C has been studied. CO_2 evolved during oxidation was measured using an infra-red gas analyzer. The presence of C lowers the oxidation rate relative to that of pure Fe and this has been related to the rejection of carbon at the alloy/scale interface causing poor contact between scale and alloy. As a result, the scale contains a higher proportion of magnetite, which reduces its overall growth rate. Very little carbon is lost to the atmosphere. The ease with which the rejected carbon is incorporated into the alloy depends on the alloy structure.

Present addresses: [+]Chemistry Section, Z. H. College of Engineering and Technology, Aligarh Muslim University, Aligarh, India.

Keyworks: iron-carbon, oxidation, decarburization.

INTRODUCTION

Many studies have been carried out on the effects of carbon on the oxidation behavior of iron, but almost exclusively steels have been used. Steels have the disadvantage that the presence of other alloying elements also participate in the scaling reaction, making interpretation difficult. In early studies (1-4) the irregular behavior of Fe-C alloys was attributed to the development of appreciable pressures of CO and CO_2 beneath the scale when the carbon in the alloy is oxidized. This in turn leads to the breakdown of otherwise protective scales by the formation of cracks and blisters. However, relatively few systematic studies have been carried out and the precise role of C is ill-defined.

Engell and Peters (5) and Engel and Bohenkamp (6, 7) suggested that the oxidation of C takes place at the metal/scale interface without scale rupture, and the oxidation proceeded according to a parabolic rate law. Decarburization occurred during oxidation and it was concluded that formation of pores in the scale permitted effusion of the gaseous oxides of C. They further proposed that the pores offered a constant resistance to gas flow at all times so that O_2 could not be directly transported from the gas phase to the metal surface, but rather reacted with CO within the pores to produce CO_2, some of which then reacted with C arriving at the base of the pores to produce more CO.

Similar studies by Manenc and co-workers (8-12) in the temperature range 740°-900°C indicated that decarburization only occurred where the surface scale was poorly adherent to the metal, this being identified by formation of greater proportions of the higher oxides of Fe, Fe_3O_4 and Fe_2O_3, than would be expected. Where an adherent scale formed, carburization took place. Again, they concluded that decarburization must take place via microcracks in the scale, and not by solid state transport: the solubility of carbon in FeO is very low, being 2-5 x 10^{-5} wt.% at 750°C (9,13) and $\sim$ 6 x 10^{-4} wt.% at 800°C(13).

More recently, Caplan et al. (14) found that the oxidation rate of Fe-0.5 and 1.0 wt% C alloys was considerably slower than that of pure Fe at 1 atm. O_2

and 700°C, but not at 500°C (15). The oxide scale contained little or no FeO and was poorly adherent. A thin film of graphite was identified at the metal-oxide interface and it was suggested that this film caused the abnormally slow oxidation rate.

In view of the somewhat conflicting results referred to above, the present study attempts to monitor the oxides of carbon, if any, evolved during the oxidation of Fe-C alloys.

EXPERIMENTAL

The alloys were prepared by melting in a high frequency induction furnace under a vacuum of 10^{-4} to 10^{-5} Torr followed by casting into rectangular cross section molds. The electrolytic iron used for the preparation of the Fe-C alloys had the following analysis: C 0.01, Si 0.02, P 0.005, S 0.007, B 0.004, Cu 0.01 weight %.

The specimens used for the experiments were cut from the cast blocks to the approximate dimension 20 x 5 x 1 mm using a SiC slitting wheel. A 0.4 mm suspension hole was drilled near the middle of one end of the sample. The specimens were then abraded with 180 and 320 grade SiC papers and given a heat treatment in a vacuum furnace (approximately 10^{-6} Torr) for homogenization, removing internal stresses and producing the required structure.

Two types of heat treatments were usually carried out on the alloys, depending upon their subsequent oxidation temperature:

(i) Annealing for 4 h at 900°C (for samples to be oxidized in the range 750 to 850°C);

(ii) Annealing for 24 h at 700°C (for samples to be oxidized in the range 600 to 700°C).

After heat treatment, the specimens were abraded on 600 grade SiC paper. The specimens were then carefully washed and degreased by CCl_4 and alcohol.

The kinetic measurements were carried out using a Sartorius electronic

microbalance model 4104 coupled to a recorder; this had a sensitivity of $\pm$ 10μg.

The specimens were suspended through a quartz fibre, with a Pt loop at the end, in the reaction tube attached to the microbalance. After the balance had been poised, the hot furnace was raised around the sample and oxidation commenced. Oxidation was carried out in pure, dried oxygen at 1 atmos. pressure and a flow rate of about 100 ml/min.

The CO_2 evolved during oxidation was measured by passing the exhaust gases from the reaction tube through an Infra-Red Gas Analyser, Model 200 supplied by Analytical Development Co. The analyser was previously calibrated with Ar/CO_2 mixture containing 90 ppm CO_2, supplied by the same company. Clearly, there is some time lapse, depending on the gas flow rate through the apparatus, between the evolution of CO_2 from the sample and response of the analyser. Consenquently, the flow rate was also monitored, and found to remain constant within $\pm$ 5% during any run.

The infra-red gas analyser measures the volume of CO_2 in the gas stream in ppm, this was converted to mass of CO_2 evolved per unit area of specimen surface per unit time as a function of time, using the measured volume flow rate of gas through the microbalance. The total weight of CO_2 evolved per unit surface area was then found as a function of time by graphical integration of these rate curves.

Metallographic examination of polished cross-sections of the scale products were carried out in the conventional way. X-ray powder diffraction patterns were used in some instances to identify scale products.

RESULTS

Oxidation runs were carried out in the temperature range 600-850°C, with the main emphasis on two temperatures, 700 and 850°C. At the lower temperature the alloy structure consists of α and Fe_3C; at the higher temperature, which is above the A_3 point, the carbide would be in solution and the alloy have an α, $\alpha+\gamma$ or γ-structure depending on the carbon content.

(a) Oxidation Kinetics

Typical weight gain/time curves for the oxidation of Fe-C alloys containing 0.1, 0.4, 0.8 and 1.2 wt. % C at 850°C are shown in Figure 1. All the alloys oxidize at a much slower rate than pure Fe, a typical rate taken from a recent review by Smeltzer and Young (16) being included. The dependence on carbon content, however, is somewhat complex, with the 0.4% C alloy oxidizing at a faster rate than the other three alloys. Parabolic plots of $(\text{wt. gain})^2$ versus time are essentially linear indicating the usual diffusion-controlled growth of the iron-oxide scale. However, with the 1.2% C alloy, there is an abrupt change of slope, towards a higher oxidation rate after about 6h oxidation. As indicated later, the decarburization rate curves show higher carbon losses during the initial period for this alloy, which could represent poor contact between metal and scale due to rapid evolution of CO_2. After 6h, the rate of carbon loss dropped considerable. Loss of carbon as gaseous oxides represents a virtually insignificant weight loss.

Similar parabolic kinetics were observed at 700°C, and are shown in Figure 2, a typical curve for pure Fe at this temperature being included (16). Table I summarizes the parabolic rate constants at the two temperatures. At 700°C, the rates for the 0.1, 0.4 and 0.8% C alloy are similar, but that of the 1.2% C alloy is considerably higher; at 850°C there is a more gradual increase in parabolic rate constant with carbon content, except for the 0.4% C alloy, which has an exceptionally high rate, as referred to earlier.

Parabolic rates were generally observed at other temperatures in the range 600-800°C, with the rates gradually incrasing with temperature as might be expected. However, there was a sudden increase in rate at 850°C, compared to 800°C, producing an apparent break in the Arrhenius plot, which might be attributable to the phase changes in the alloy, as discussed later.

(b) Kinetics of Decarburization During Oxidation

The kinetics of decarburization during oxidation were measured by simultaneously analyzing the exhaust gases from the thermobalance for CO_2 as described earlier. The rate of decarburization (or carbon loss) is expressed in terms of weight loss of carbon per unit surface area of sample per unit time and is calculated from the CO_2 content of the exhaust gases and the volume flow rate normalized to unit surface area of the sample. Figure 3 shows decarburization rate curves at 850°C. In all cases, the rate of carbon loss falls with time following an initially rapid rate during the first 5 min. or so of oxidation. The initially high rates of CO_2 evolution are apparently genuine, and not associated with the oxidation of any hydrocarbon contamination remaining on the sample surface after the cleaning operations since no CO_2 was detected when a carbon-free alloy was given an identical treatment. The rate curves indicate relatively higher carbon losses from the 1.2% C alloy in comparison to the other alloys, which all tend to have fairly similar loss rates. The 1.2% C alloy shows a rapid carbon loss for a period of about 6h, and then the rate becomes almost constant. On the other hand, the 0.4% C alloys shows high carbon losses only for a period of less than 1h, followed by carbon losses of extremely low concentrations (about 2 ppm CO_2 is measured corresponding to a rate of 0.05μg/cm^2/min.). Figure 4 presents the total carbon loss as a function of time at 850°C, obtained by integrating Figure 3. Because of the very low rates involved - the highest total loss observed is only 10.2μg/cm^2 after 24h oxidation - it is difficult to identify any particular rate law: a diffusion-controlled rate would be anticipated.

There is no measurable carbon loss during oxidation at 700°C. With the 1.2% C alloy, CO_2 is evolved to the extent of 10-15 ppm (0.5 to 0.75μg/cm^2/min.) for 5 to 10 min. initially, but then it ceases.

(c) Morphology of the Oxide Scales

Debye-Scherrer x-ray diffraction patterns of the scales indicated all three oxides of iron were present. In general, the outer scale layer consisted of haematite, followed by magnetite and the innermost layer being wustite. With pure iron, these three phases form three well-defined, parallel-sided layers, with magnetite and haematite accounting for approximately 5% of the total scale thickness at temperatures of 700°C and above. However, this balance is disturbed by the presence of carbon in the alloy and indeed the scale layers are very much less regular in thickness and are often highly porous.

The scale on the 0.1% C alloy, which had the slowest oxidation rate at 850°C, had a high proportion of magnetite in the middle layer. In contrast, the Fe-0.4% C alloy, the predominant phase was wustite, as it is with pure Fe: Figure 5(a). The 1.2% C alloy had the highest concentration of voids in the scale, Figure 5(b), which is presumably due to the rapid and higher carbon losses during oxidation. The oxidized specimens, when etched with nital showed a dispersion of cementite in the alloy matrix. In some cases, notably the 0.1 and 0.8% C alloys, there was evidence of carbon loss during oxidation, however, this was not very evident with the 0.4 and 1.2% C alloys.

(d) Oxidation of Decarburized Alloys

In order to understand more fully the effect of carbon on the oxidation behavior, all the alloys were decarburized for 1h in wet hydrogen at 850°C, and then oxidized at the same temperature. Table II indicates the depth of the decarburized zone for the four carbon-containing alloys: the depths were calculated from weight change data which is included in Figure 6. The weight loss during decarburizing increases with increasing carbon content as might be expected.

Decarburization produces a zone of virtually carbon-free ferrite at the alloy surface, overlying the austenitic Fe-C solution. Thus, initially oxidation should be expected to produce oxide scales typical of pure Fe, until the decarburized layer has been completely oxidized. The time at which this occurs depends on the thickness of the decarburized layer, and hence on the duration of the initial decarburization period.

Figure 6 presents weight gain/time data for the decarburized alloys where the weight gain is virtually independent of the original alloy carbon content. Parabolic rate constants are presented in Table II and compared with those obtained for the undecarburized alloys. In all cases, there is a very significant increase in rate constant by an order of magnitude or more. The rate constants for oxidation, of the decarburized alloys are similar to that expected for pure iron at this temperature typically $1.0 \times 10^{-8}\ g^2cm^{-4}s^{-1}$. Furthermore, the rate constants for the 0.4 and 0.8% C alloys increases further with increasing decarburization time as indicated in Table II.

Table II also includes the displacement of the alloy/scale interface after oxidation which has been calculated from the weight change data. In all cases, this is less than the calculated thickness of the decarburized layer and thus this will not be completely consumed during the oxidation process. In fact, extrapolation of plots of the displacement of the alloy/scale interface as a function of time indicate that exposure times of 40.5, 10.8, 8.9 and 5.4h would be required to completely oxidize the decarburized layer produced by 1h in wet hydrogen for the 0.1, 0.4, 0.8 and 1.2% C alloys respectively. However, even though the decarburized layer is not completely consumed, during oxidation carbon can diffuse through the decarburized surface layer to the alloy/scale interface and interact with the oxidation process. Figure 7 shows the increased carbon

evolution as a function of time during the oxidation of the decarburized alloys. The total carbon loss during the 5h oxidation can be calculated by graphical integration of these curves and is 0, 2.2, 5.9 and 3.2 μg for the 0.1, 0.4, 0.8 and 1.2% C alloys respectively; corresponding values for the undecarburized alloys for the same oxidation time are 1.6, 0.6, 1.4 and 2.6 μg respectively. The higher carbon losses from the decarburized alloys in comparison to the undecarburized alloys is related to the higher oxidation rates of the material in the decarburized conditions.

(e) Morphology of the Decarburized and Oxidized Alloys

Figure 8 shows a cross-section of the 0.1% C alloy decarburized for 1h followed by 5h oxidation at 850°C. As might be anticipated, the scale is typical of that formed on pure Fe and consists of a uniform, three-layered scale of haematite, magnetite and wustite. The scale on the 0.4% C alloy is very similar. However, with the 0.8 and 1.2% C alloys, Figure 9 shows a typical example, the relative thickness of the magnetite layer is somewhat greater than would be expected for pure Fe, or indeed found in the two more dilute C alloys. This also accounts for the smaller parabolic rate constants of oxidation of the 0.8 and 1.2% C, and is related to the interference of C with the oxide growth rate, evolution of CO_2 presumably causing porosity and poor contact between scale and metal. As indicated earlier, the depth of carburization produced by 1h in wet H_2 decreases with increasing carbon content of the alloy. Indeed, after the 5h oxidation, the decarburized layer has been virtually all consumed in the 1.2% C alloy.

DISCUSSION

The effect of carbon is to reduce the oxidation rate of pure Fe. The scale formed is over-oxidized, containing higher proportions of magnetite and haematite than are present in the scales formed on pure iron. The variation

in parabolic rate constant of oxidation with relative thickness of the various oxide layers can be calculated approximately following the analysis of Yurek et al. (17). For simplicity, it is assumed that only FeO and Fe_3O_4 form. Then, the overall parabolic rate constant, $Kp(cm^2/s)$ is given by

$$Kp = \frac{(1+\eta/\xi)^2}{1+\delta\eta\ V_{FeO}/\nu\xi V_{Fe_3O_4}}\ Kp(FeO) = \frac{1+\xi/\eta)^2}{1+\xi\ V_{Fe_3O_4}/\eta\ V_{FeO}}\ Kp(Fe_3O_4)$$

where Kp(FeO) and $Kp(Fe_3O_4)$, ξ and η, V_{FeO} and $V_{Fe_3O_4}$ and ν and δ are the individual parabolic rate constants, the thicknesses, molar volumes and metal/oxygen ratios of wustite and magnetite respectively. According to Paidassi (18), at 850°C for the oxidation of pure iron, the relative thickness of the magnetite is about 4%, that is η/ξ has a value of about 0.041. In the over-oxidized scales, the growth rate of magnetite, Kp (Fe_3O_4), should not be altered, since the oxygen potentials at its inner interface with FeO and its outer interface with haematite are the same. Thus, the ratio of overall growth rate of the overoxidized scale, K_p', to that of the scale which normally grows on Fe, Kp, is given by

$$K_p'/K_p = \frac{(1+\xi/\eta)^2}{1+\xi V_{Fe_3O_4}/\eta V_{FeO}}$$

Using values for the molar volumes of Fe_3O_4 as 11.2 and 11.7 cm^3/mole respectively, the ratio of parabolic rate constants for the over-oxidized scale to that which normally grows on iron can be calculated as a function of the relative thickness of magnetite in the scale. This is presented in Figure 10, where the ratio of parabolic rate constant for the over-oxidized scale, to that normally found on pure Fe (4% magnetite at this temperature) has been used as the ordinate.

According to Figure 10, the oxidation rate can be expected to be reduced by approximately two orders of magnitude depending on the percentage of magnetite in the scale layer. This appears consistent with the observations that at 850°C the ratio of parabolic rate, constants for the undecarburized

and decarburized alloys (the latter oxidizing at the same rate as pure Fe(17)) are around 10^{-2} - 5 x 10^{-2} for the 0.1, 0.8 and 1.2% C alloys, and 10^{-1} for the 0.4% C alloy. In effect, the presence of carbon in the alloy lowers the activity of Fe at the inner surface of the scale to the point where magnetite is the stable phase. It has been suggested that upon oxidation carbon is rejected from the alloy and forms a thin layer of graphite at the alloy/scale interface (14). Although this has not been demonstrated in the present work, analyses of the exhaust gases from the thermobalance during oxidation have indicated that little of the carbon from the alloy is oxidized. Table III compares the expected loss of carbon, calculated by assuming the total carbon contained in the volume of alloy converted into oxide (using the measured parabolic rate constant), with that measured experimentally in a 24h period. The % of the carbon actually lost is very small for each alloy. Surprisingly, however, there is no real evidence of carburization of the alloy at the alloy/scale interface, although carbon diffusion in the alloy at this temperature is relatively rapid, and it is quite possible that the carbon has been redistributed throughout the whole sample section, which would not change the overall composition by very much.

The decrease in oxidation rate of the Fe-C alloys, then, is clearly related to some modification ot the alloy/scale interface and the development of a film of graphite, referred to above, is one possibility. Alternatively, it may be due to general loss of contact between scale and alloy, aided by the formation of CO and CO_2 at the interface, although it has been clearly shown that these gaseous oxides do not escape through the scale. There is a general tendency for the oxidation rate to increase with increasing carbon content of the alloy, except that the Fe-0.4% C alloy is anomalous in this respect, with a much higher rate than either the 0.1 or 0.8% alloys. Clearly the alloy structure is important. At 850°C the 0.1% alloy consists of the $\alpha+\gamma$ phases, the 0.4 and 0.8% alloys of the γ-phase, and the 1.2% alloy, $\gamma+Fe_3C$.

It is presumably easier for rejected carbon to be incorporated into the 0.4% C alloy since the γ-phase is considerably undersaturated with respect to carbon. There is thus less separation of the scale from the alloy, less magnetite in the scale, and consequently a higher overall oxidation rate. Although, the 0.8% alloy also consists of γ, it is relatively close to the saturation limit. The 0.1 and 1.2% C alloys already contain, at least, one phase which is saturated with carbon and thus can only accommodate excess carbon by changing the relative proportions of the two phases. If the higher oxidation rate of the 1.2% C alloy relative to the 0.1% alloy is significant, this implies that it is easier to form Fe_3C from saturated γ than γ from saturated α.

ACKNOWLEDGEMENTS

This work was carried out whilst the authors were at the University of Liverpool and one of us (AVM) acknowledges the award of a research studentship. The work is being published with the support by the Director, Office of Energy Research, Office of Basic Energy Sciences, Materials Sciences Division of the U.S. Department of Energy under Contract Number W-7405-ENG-48.

REFERENCES

1. E. Portevin, E. Pretet and H. Jolivet, Rev. Metall., 31, 101, 186, 219 (1934).

2. C. Upthegrove and D. Murphy, Trans. Amer. Soc. Steel Treatment, 21, 73 (1933).

3. C. A. Siebert, Trans. Amer. Soc. Metals, 27, 75 (1939).

4. D. J. McAdam and G. W. Geil, J. Res. Nat. Bur. Stand., 23, 63 (1939).

5. H. J. Engel and F. K. Peters, Arch. Eisenhuttenw., 28, 567 (1957).

6. K. Bohenkamp and H. J. Engel, Arch. Eisenhuttenw., 32, 359 (1962).

7. K. Bohenkamp and H. J. Engel, Proc. 1st Int. Congress on Metallic Corrosion, p. 125, Butterworths (1962).

8. J. Manenc, M. Bojic and J. Benard, C. R. Acad. Sci., Paris, 264, 1573 (1967).

9. J. P. Plumensi, A. Kohn, G. Vagnard and J. Manenc, Corros. Sci., 9, 309 (1969).

10. J. Manenc and G. Vagnard, Corros. Sci., 9, 857 (1969).

11. J. Baud, J. P. Plumensi and J. Manenc, Werkst. Korros., 23, 876 (1972).

12. J. Baud, A. Ferrier, J. Manenc and J. Benard, Oxid. Met., 9, 69 (1975).

13. H. Meurer and H. Schmalzried, Arch. Eisenhuttenw., 42, 87 (1971).

14. D. Caplan, G. I. Sproule, R. J. Hussey and M. J. Graham, Oxid. Met., 13, 255 (1979).

15. D. Caplan, G. I. Sproule, R. J. Hussey and M. J. Graham, Oxid. Met., 12, 67 (1978).

16. W. W. Smeltzer and D. J. Young, Prog. in Solid State Chem. (1975) 17.

17. G. J. Yurek, J. P. Hirth and R. A. Rapp, Oxid. of Metals 8 (1974) 265.

18. J. Paidassi, Rev. Metall. 54, 569 (1957).

TABLE I

PARABOLIC RATE CONSTANTS FOR THE OXIDATION OF Fe-C ALLOYS AT 700 and 850°C

	Parabolic Rate Constant, $g^2\ cm^{-4}\ s^{-1}$	
	700°C	850°C
Fe-0.1% C	6.1×10^{-11}	1.2×10^{-9}
Fe-0.4% C	8.6×10^{-11}	1.6×10^{-8}
Fe-0.8% C	5.2×10^{-11}	3.3×10^{-9}
Fe-1.2% C	1.8×10^{-10}	7.9×10^{-9}

TABLE II

OXIDATION OF DECARBURIZED Fe-C ALLOYS AT 850°C

Alloy	Decarburization Time, h	Decarburized Layer Thickness μm	Oxidation Time h	Alloy/Scale Int. Displacement μm	Parabolic Rate Constant, $g^2/cm^4/s$	
					Decarb.	Undecarb.
Fe-0.1% C	1	495	5	171	1.0×10^{-7}	1.2×10^{-9}
Fe-0.4% C	1	272	5	176	8.8×10^{-8}	1.6×10^{-8}
Fe-0.4% C	2	367	3	161	1.3×10^{-7}	1.6×10^{-8}
Fe-0.8% C	1	191	5	143	6.3×10^{-8}	3.3×10^{-9}
Fe-0.8% C	4	388	4	181	1.2×10^{-7}	3.3×10^{-9}
Fe-1.2% C	1	171	5	143	8.3×10^{-8}	8.0×10^{-9}

TABLE III

TOTAL CARBON LOSS DURING OXIDATION OF Fe-C ALLOYS AT 850°C

	Total Carbon Loss In 24th Oxidation		
	Calculated From Metal Loss Data $\mu g/cm^2$	Experimental $\mu g/cm^2$	c/o Total Carbon Actually Lost
Fe-0.1% C	38	3.4	8.9
Fe-0.4% C	510	1.6	0.3
Fe-0.8% C	480	4.0	0.8
Fe-1.2% C	980	10.2	1.0

FIGURE CAPTIONS

Figure 1. Weight gain/time curves for Fe-C alloys oxidized at 850°C.

Figure 2. Weight gain/time curves for Fe-C alloys oxidized at 700°C.

Figure 3. Decarburization rate curves for Fe-C alloys during oxidation at 850°C.

Figure 4. Total carbon loss as a function of time for Fe-C alloys oxidized at 850°C.

Figure 5(a). Cross-section of the scale formed on Fe-0.4% C oxidized for 5h at 850°C.

Figure 5(b). Cross-section of the scale formed on Fe-1.2% C oxidized for 5h at 850°C.

Figure 6. Weight change data for the decarburization and oxidation of Fe-C alloys at 850°C.

Figure 7. Carbon evolution as a function of time during the oxidation of decarburized Fe-C alloys at 850°C.

Figure 8. Cross-section of Fe-0.1% C decarburized for 1h followed by 5h oxidation at 850°C.

Figure 9. Cross-section of Fe-1.2% C decarburized for 1h followed by 5h oxidation at 850°C.

Figure 10. Effect of magnetite layer on the oxidation rate of iron at 850°C.

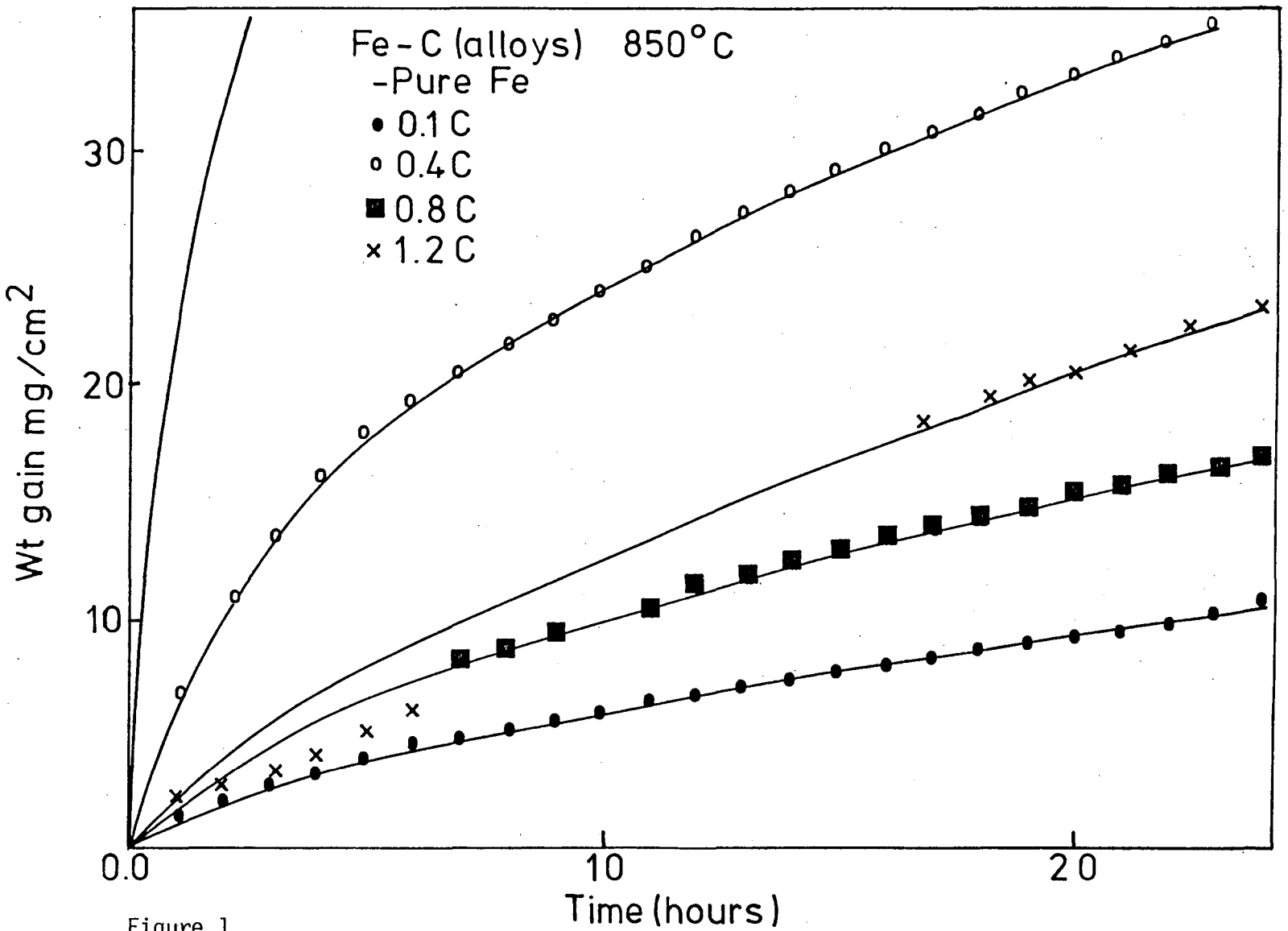

Figure 1.

XBL 815-9979

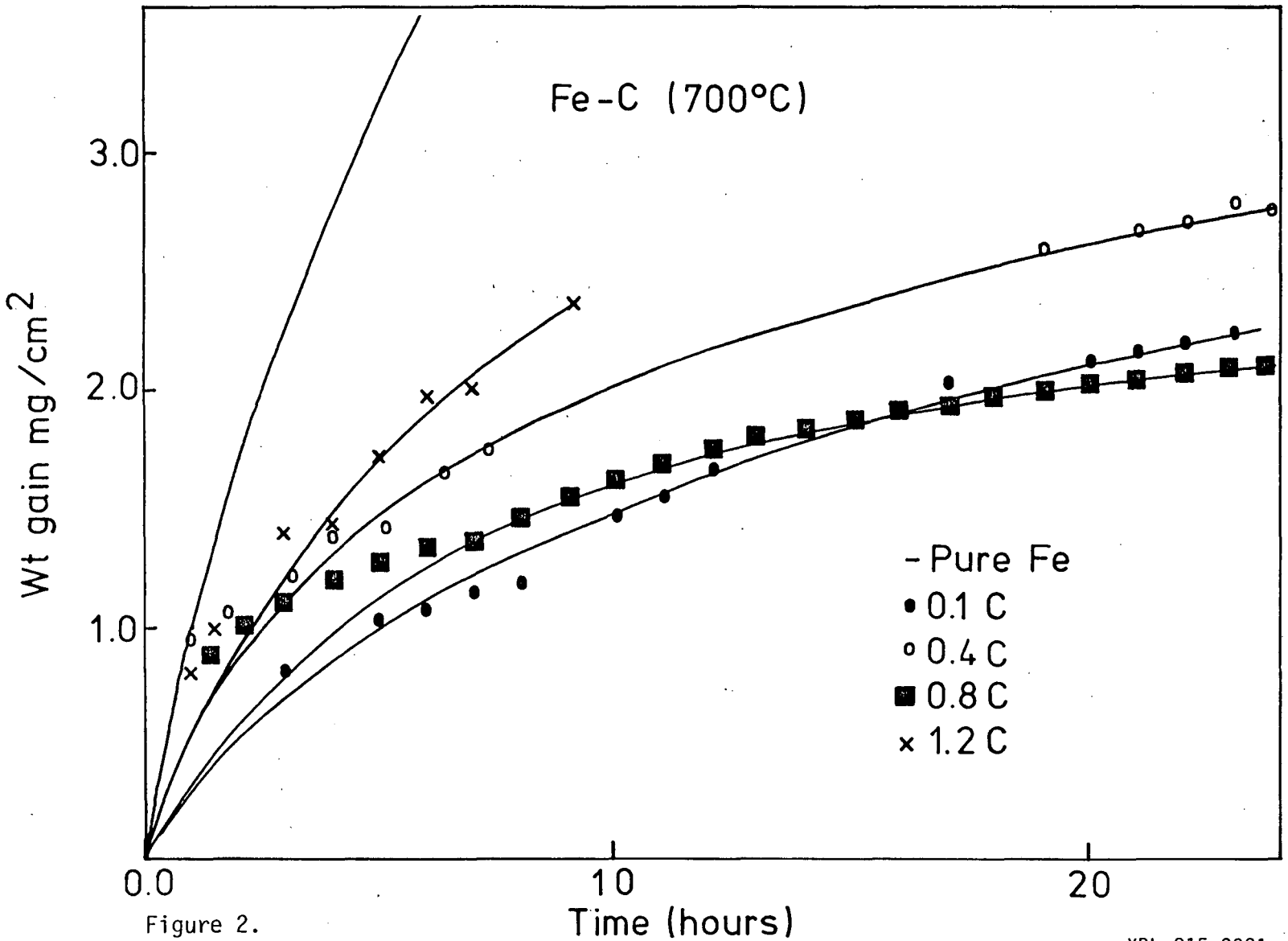

Figure 2.

XBL 815-9981

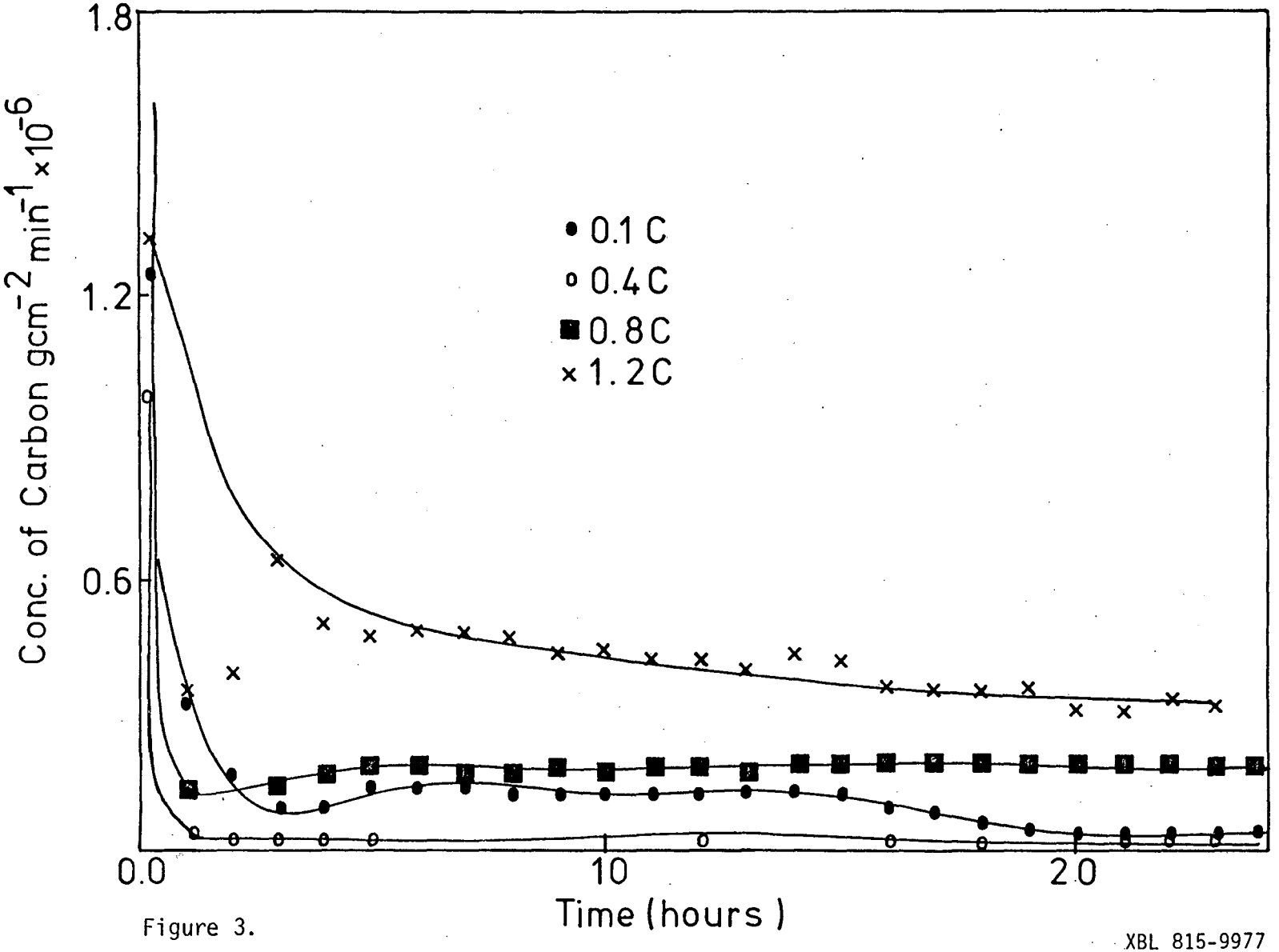

Figure 3.

XBL 815-9977

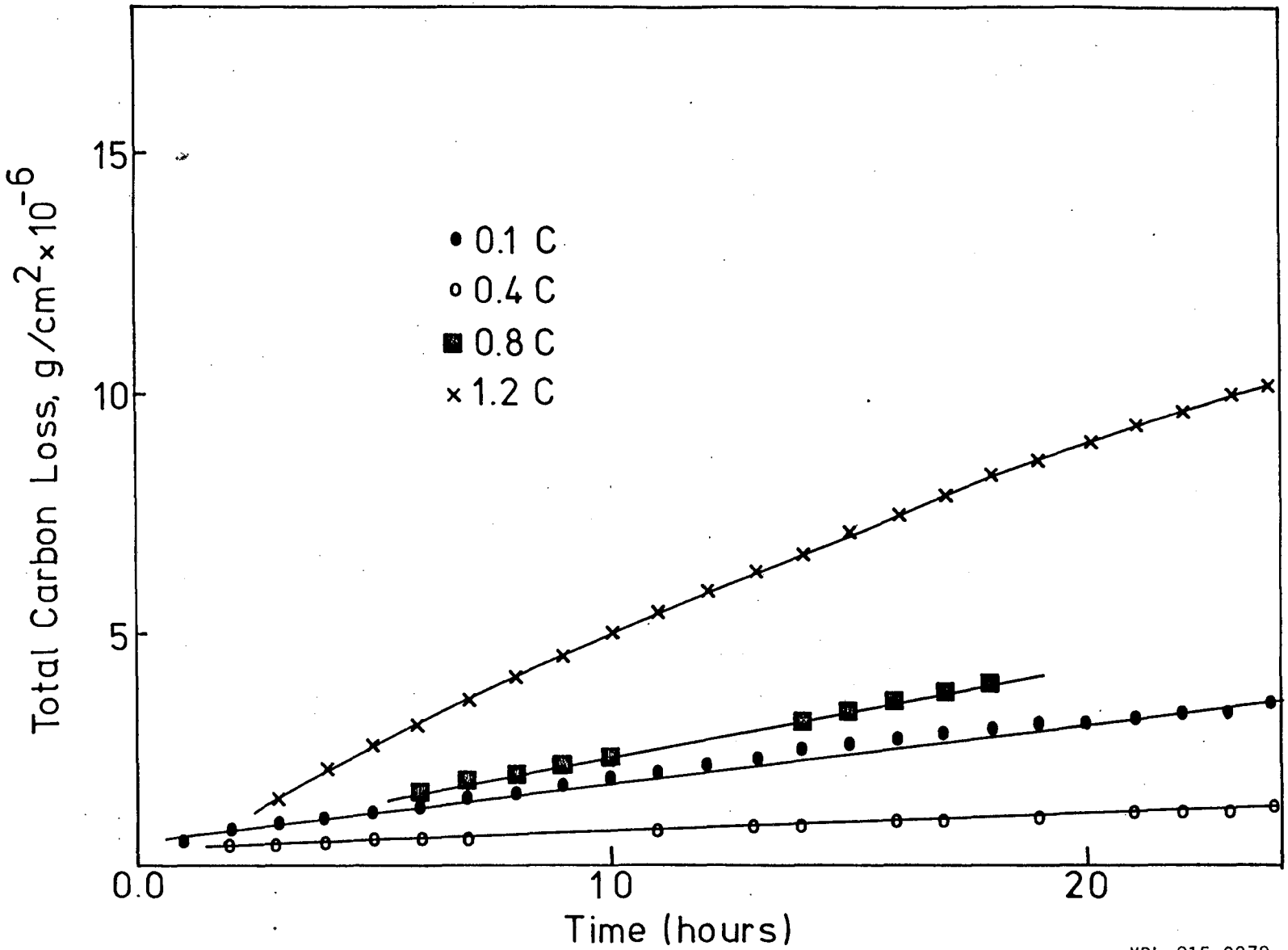

Figure 4.

XBL 815-9978

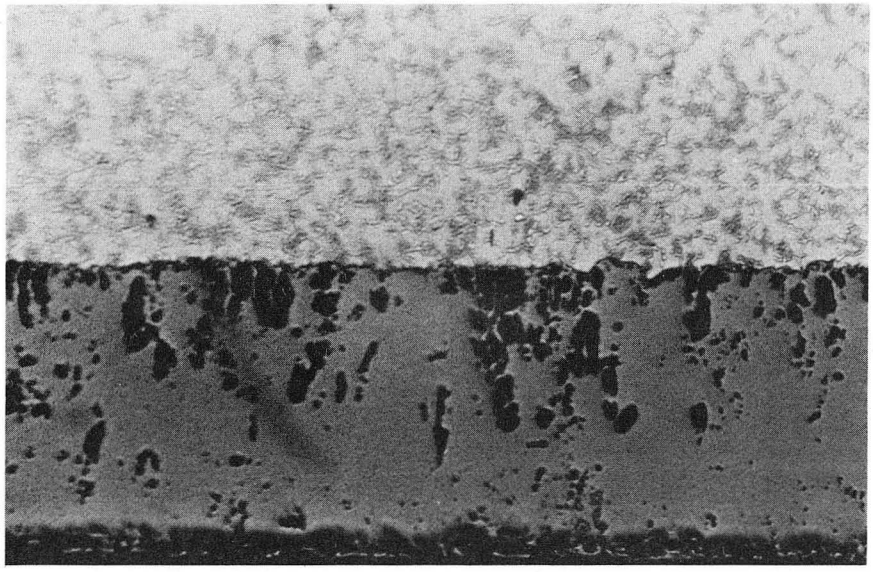

Figure 5a. XBB815-4103

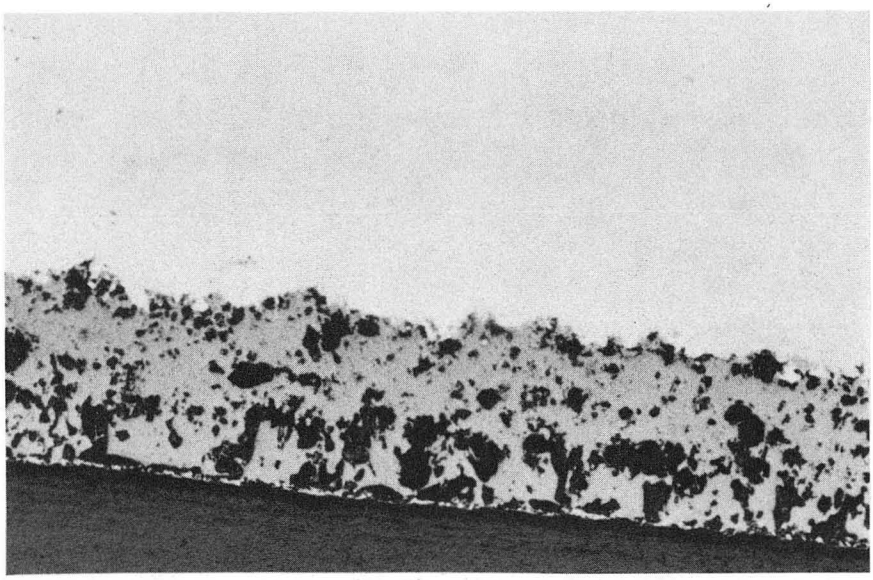

Figure 5b. XBB815-4104

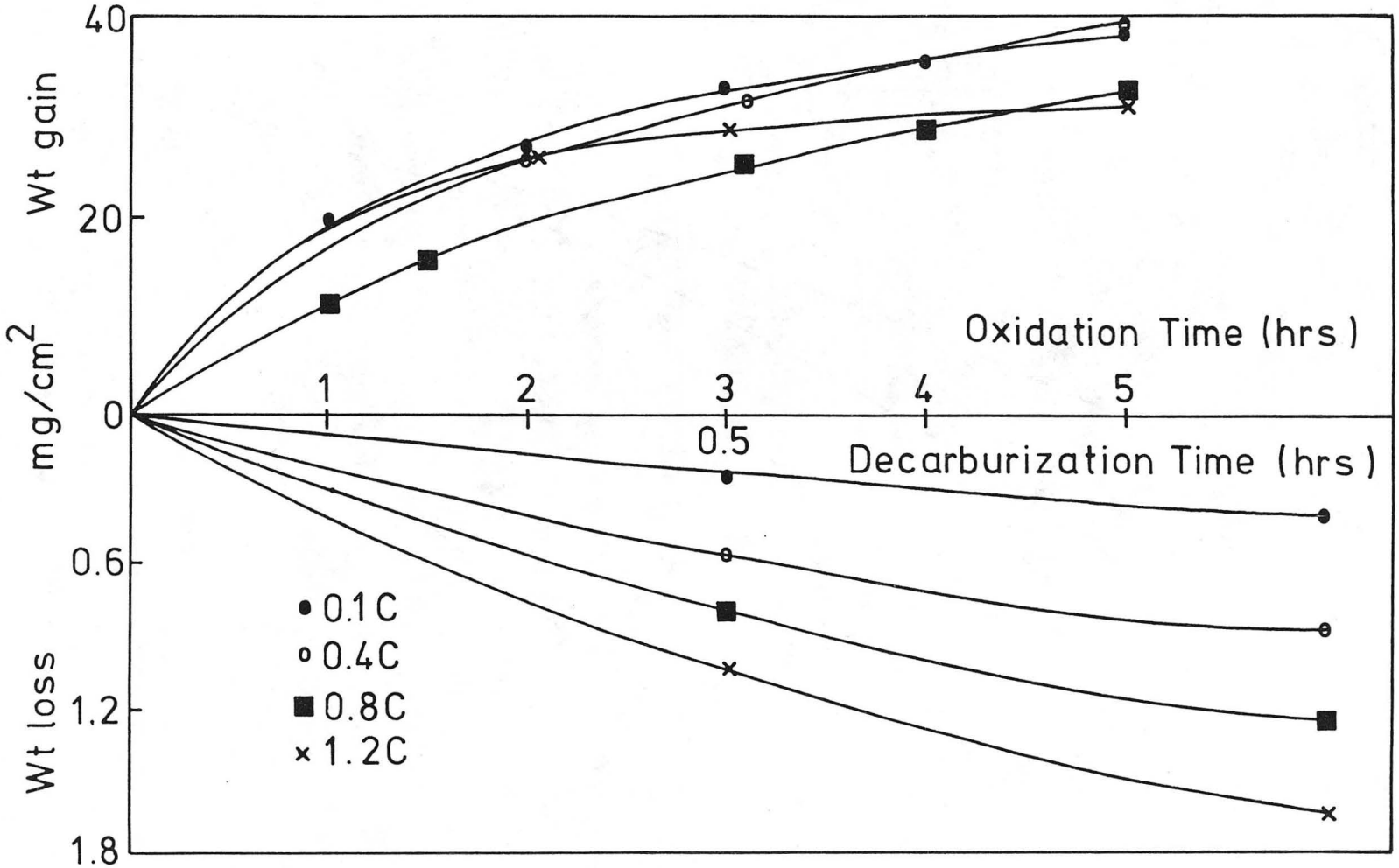

Figure 6.

XBL 815-9982

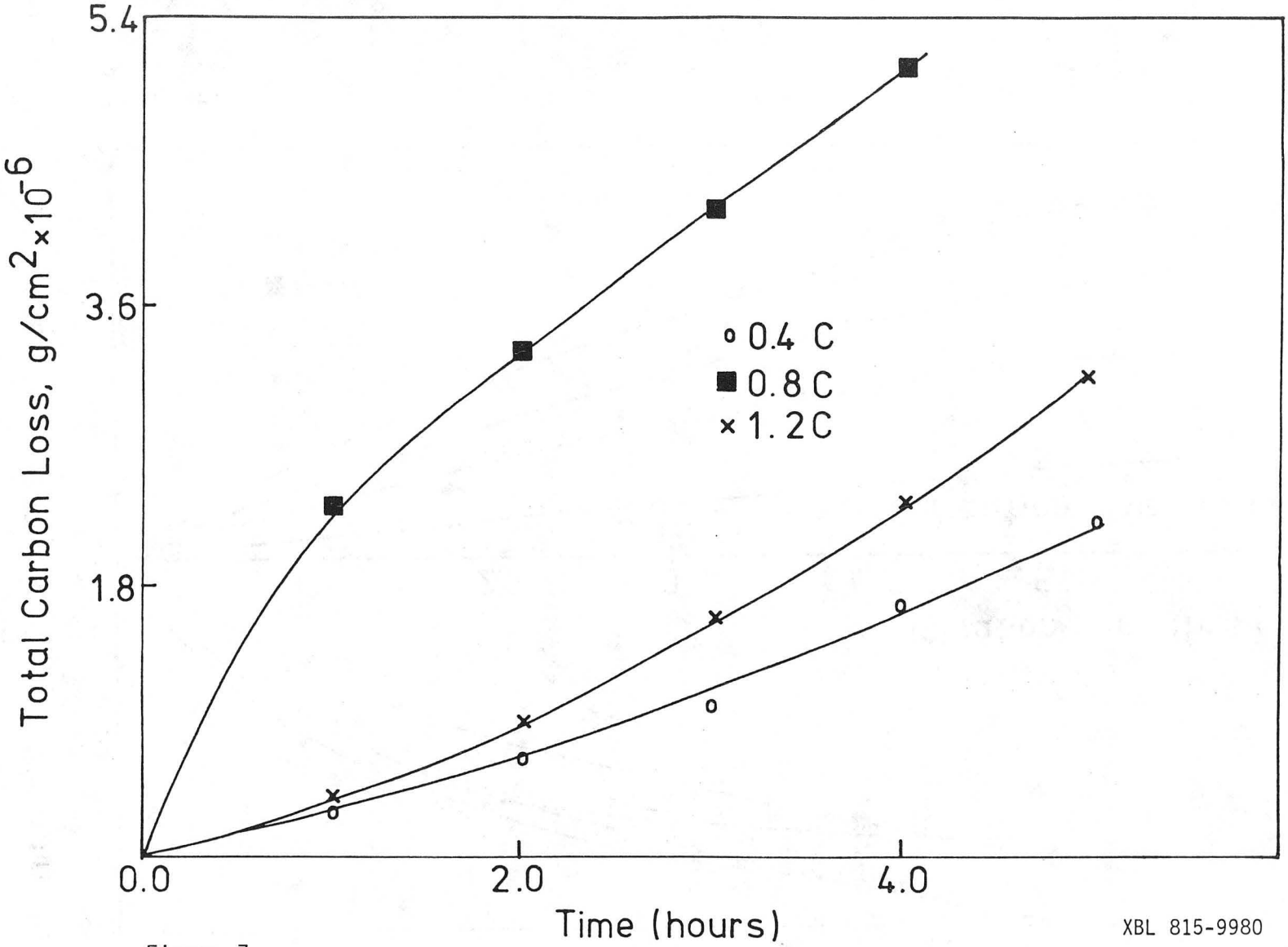

XBL 815-9980

Figure 7.

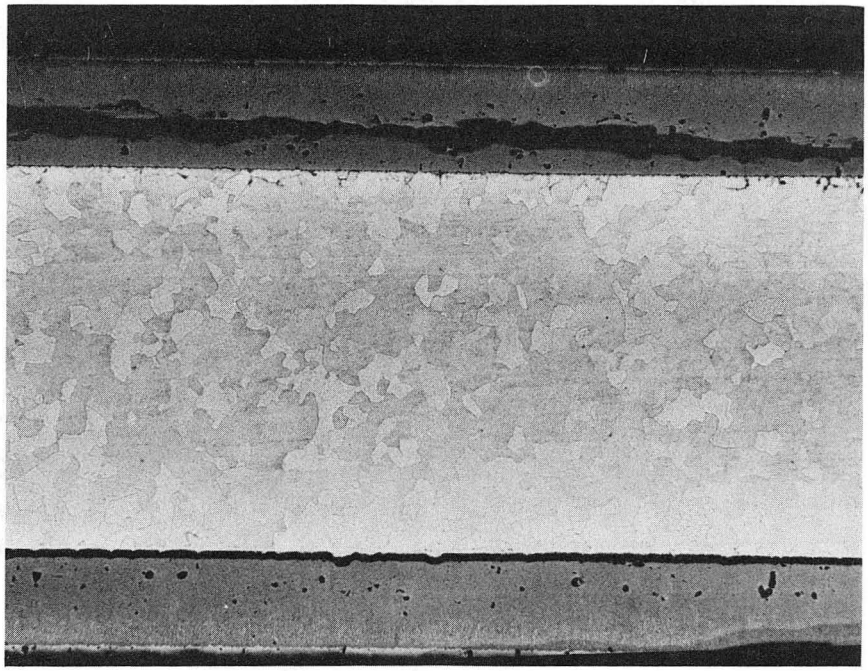

Figure 8. XBB 815-4101

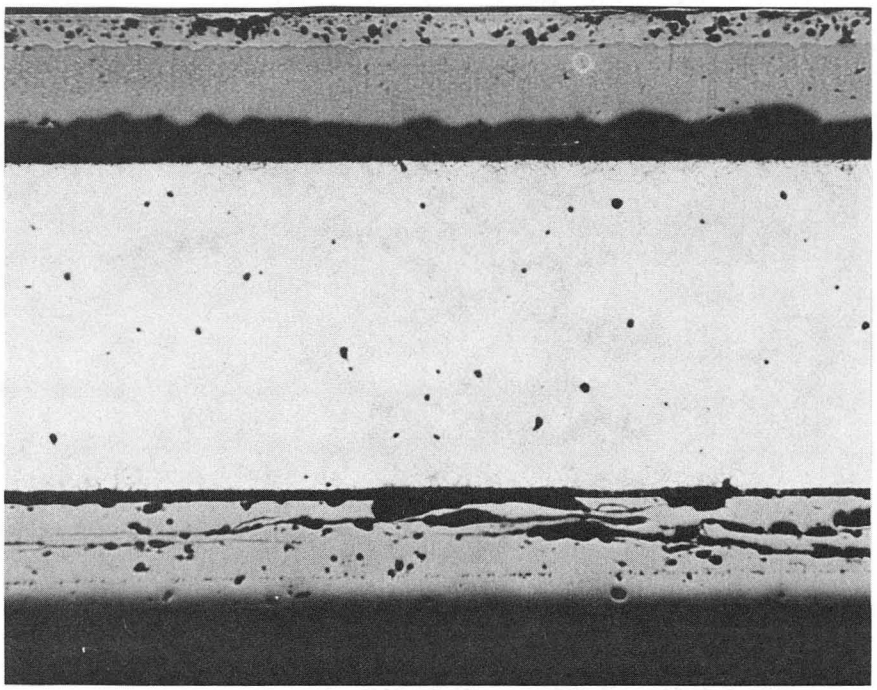

Figure 9 XBB815-4102

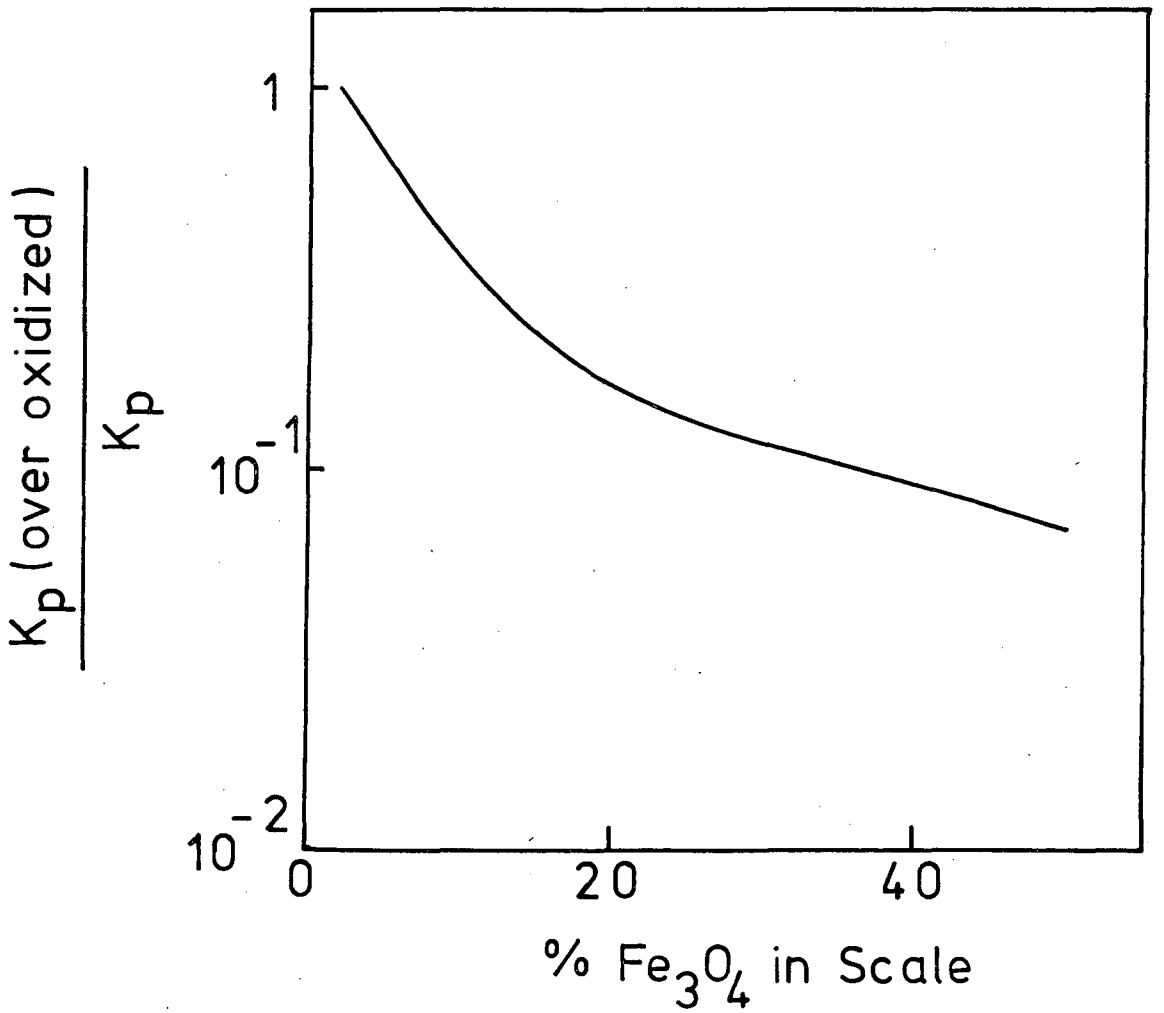

Figure 10. XBL 815-9983

This report was done with support from the Department of Energy. Any conclusions or opinions expressed in this report represent solely those of the author(s) and not necessarily those of The Regents of the University of California, the Lawrence Berkeley Laboratory or the Department of Energy.

Reference to a company or product name does not imply approval or recommendation of the product by the University of California or the U.S. Department of Energy to the exclusion of others that may be suitable.

TECHNICAL INFORMATION DEPARTMENT
LAWRENCE BERKELEY LABORATORY
UNIVERSITY OF CALIFORNIA
BERKELEY, CALIFORNIA 94720